SUPPLEMENTAL MATERIAL

Ventricular cardiomyocyte strand models. The *Fhf2*^{WT} and *Fhf2*^{KO} ventricular cardiomyocyte models described previously[1] were scripted onto the NEURON software platform[14] with several modifications and then linked into strands with gap junctional conductances.

Cardiomyocyte Dimensions and Gap Junction Connectivity into Strands: The cardiomyocyte model cells (myocite.hoc) are cylinders with length (cell.L) of 100 microns and diameter (cell.diam) of 22.34 microns. With standard membrane unit capacitance (cell.cm) of 1 μF/cm^2, each cell's membrane capacitance is 70 pF. The number of cells in the strand can be selected in the Graphical User Interface (GUI); all published data analysis was on strands comprising 111 cells (1.11 cm length).

Gap junctions are modeled as reciprocal and equivalently weighted conductances between adjacent cells n and n+1. The conductance in "source" cell n is gap_sources.o[n].g, while the matching conductance in "sink" cell n+1 is gap_dests.o[n+1].g, with the currents driven by the voltage differential between source cell n and sink cell n+1. These conductances are absolute set values (in pS) multiplied by $Q10 = 1.43^{\{(^{o}C - 37)/10\}}$, unlike transmembrane ion conductances (below), which are expressed as conductance densities (S/cm^2). The normal physiological setting for junctional conductance is 772.8 nS at 37^{o}C. The junctional conductances can be manipulated equally between all cell pairs in the GUI, or specific cell pair conductances can be varied by text commands.

Ion Conductances in Cardiomyocytes: All ion conductance densities are set equivalently in all cells of the strand. Each ion conductance density can be manipulated equally throughout the strand in the GUI, or specific cell ion conductance densities can be varied by text commands.

Voltage-gated sodium conductances: The myocytes include two 16-state Markov model voltage-dependent sodium conductances termed NAV_withF and NAV_noF (Scheme 1).

Scheme 1

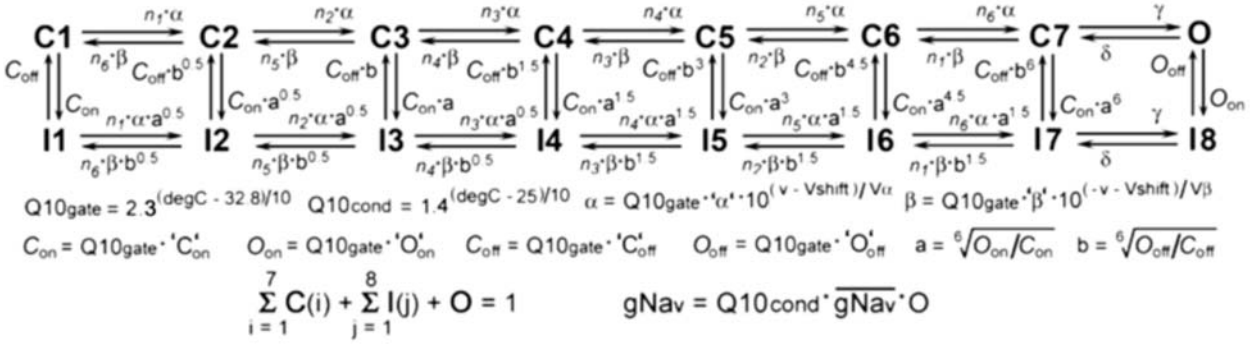

Fhf2^{KO} cardiomyocytes only have a functional NAV_noF conductance (i.e. $\overline{gNav}$ for NAV_withF = 0), while *Fhf2*^{WT} cardiomyocytes contain a mixture of NAV_withF and NAV_noF. Employing this mixture does not imply knowledge that wild-type ventricular cardiomyocytes necessarily bear a mixture of sodium channels with and without associated FHF2, but rather the mixture of models was employed to achieve a closer modeling of voltage dependent inactivation to recorded values, as presented in Online Table VII. It is also important to emphasize that for each sodium channel model, the maximum available sodium conductance upon simulated step depolarization from -135 mV to -30 mV is not equal to $\overline{gNav}$, but is equal to $\overline{gNav}$ * (C_{off}/[C_{on}+ C_{off}]). For the NAV_noF model, C_{off}/[C_{on}+ C_{off}] = 0.1667, while for the NAV_withF model, C_{off}/[C_{on}+ C_{off}] = 0.9259. Since *Fhf2*^{WT} and *Fhf2*^{KO} model cardiomyocytes were tuned to generate the same peak sodium current upon step depolarization from -135 mV, consistent with our recorded cardiomyocyte data, $\overline{gNav}$ is greater in the *Fhf2*^{KO} model cardiomyocyte. As stipulated above, that the

maximum available conductance in NAV_noF model is far less than its $\overline{gNav}$ is not meant to necessarily imply that most sodium channels in real *Fhf2*^{KO} cardiomyocytes are inactivated under all conditions.

In the Markov models, α and β are voltage(v)-dependent rate constants, Q10gate is the thermodyamic scaling factor for rate constants, and Q10cond is the thermodynamic scaling factor for conductance. Parameters with equivalent values for NAV_withF and NAV_noF models are: n1 = 100, n2 = n3 = 20, n4 = 3, n5 = 1.5, n6 = 0.75, 'α' = 2.44375 (ms^{-1}), 'β' = 0.01325 (ms^{-1}), Vα = Vβ = 9 (mV), γ = 150 (ms^{-1}), δ = 40 (ms^{-1}), 'O'$_{off}$ = 0.0005 (ms^{-1}). Parameters with different values for NAV_withF vs NAV_noF models are: 'C'$_{on}$ = 0.004 *vs* 0.025 (ms^{-1}), 'C'$_{off}$ = 0.05 *vs* 0.005 (ms^{-1}), 'O'$_{on}$ = 0.85 *vs* 1.3 (ms^{-1}), V_{shift} = -54 *vs* -57.5 (mV). In the *Fhf2*^{KO} cardiomyocyte, $\overline{gNav}$_noF = 25 nS/pF, while in the *Fhf2*^{WT} cardiomyocyte, $\overline{gNav}$_noF = 8.83 nS/pF and $\overline{gNav}$_withF = 2.94 nS/pF.

Online Table VII presents the Nav inactivation and activation characteristics and generated currents of the *Fhf2*^{WT} and *Fhf2*^{KO} cardiomyocyte models, which are in close agreement with sodium current recordings from *Fhf2*^{WT} and *Fhf2*^{KO} ventricular cardiomyocytes[1, 2] (and this paper). The $\overline{gNav}$ densities for the *Fhf2*^{WT} cardiomyocyte were estimated to generate action potential amplitude in isolated cardiomyocyte model with amplitude similar to prior recordings and conduction velocity in model strand comparable to velocity reported by optical mapping, while $\overline{gNav}$ for NAV_noF in *Fhf2*^{KO} cells allowed *Fhf2*^{WT} and *Fhf2*^{KO} model cardiomyocytes to generate same peak sodium current upon depolarization from -135 mV holding potential, as previously demonstrated empirically[1]. A third cardiomyocyte model termed *Fhf2*^{WT}*Na*$_V^{HYPO}$ has the same Nav gating parameters as the *Fhf2*^{WT} model, but the Nav densities are reduced by a factor of 0.49 so that the *Fhf2*^{WT}*Na*$_V^{HYPO}$ and *Fhf2*^{KO} models generate the same I-Na$_{peak}$ when depolarized from a -87mV holding potential (Online Table VII).

Nomenclature clarification: The names of rate parameters with units ms^{-1} above that are flanked by apostrophes are named differently in the uploaded Nav models, where the rate parameters are instead preceded by the prefix A. As examples, 'α' in the publication is equivalent to Aα in the uploaded model, 'C'$_{off}$ is equivalent to AC$_{off}$, etc. Additionally, $\overline{gNav}$ in the publication is equivalent to gnabar in the uploaded model.

Voltage-gated calcium conductance: *Fhf2*^{WT} and *Fhf2*^{KO} cardiomyocyte models now have an equivalent L-type voltage-gated calcium conductance expressed through an 8-state Markov model (Scheme 2) based upon the equivalent calcium current density, voltage dependence of activation and steady-state inactivation, and voltage-dependent rate of inactivation measured empirically in *Fhf2*^{WT} and *Fhf2*^{KO} cardiomyocytes (Figure 2 and Table 1).

Scheme 2

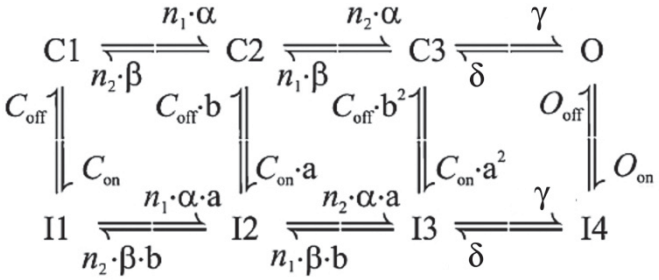

The kinetic parameters are: Q10 = $3^{\{(^{o}C - 32.76)/10\}}$, α = Q10 * 11.74 * $10^{\{(V_m + 17)/50\}}$ (ms^{-1}), β = Q10 * 0.0324 * $10^{\{(-V_m - 17)/5.5\}}$ (ms^{-1}), n_1 = 32.532, n_2 = 0.123, γ = Q10 * 150 (ms^{-1}), δ = Q10 * 40 (ms^{-1}), C_{on} = Q10 * 0.001 (ms^{-1}), C_{off} = Q10 * 10 (ms^{-1}), O_{on} = Q10 * 0.2 (ms^{-1}), O_{off} = Q10 * 0.001 (ms^{-1}), a = $(O_{on}/C_{on})^{0.5}$, b = $(O_{off}/C_{off})^{0.5}$, where V_m is membrane voltage.

Potassium conductances: The potassium conductances are taken from Bondarenko et al.[15] and include the time-dependent conductances fast transient outward conductance (g_Kto_f), noninactivating ultrarapid delayed rectifer (g_Kurdr), noninactivating rapid delayed rectifier (g_Krdr), noninactivating slow delayed

rectifier (g_Ksdr), and steady-state conductance (g_Kss), along with time-independent conductance (g_Kti) that has both leak and inward rectifier components. The weights of these conductances were adjusted 1) to give passive property ΔV as function of injected current similar to empirically recorded dissociated ventricular cardiomyocytes[1], and 2) to give a decay in the action potential in cardiomyocyte strand models similar to measured action potential decay optically recorded in paced ventricular myocardium (Online Fig II). These conductance values (S/μF) are g_Kti = 0.00021, g_Kss = 0.00007, g_Kto_f = 0.0000235, g_Kurdr = 0.000025, g_Krdr = 0.000468, g_Ksdr = 0.00000575.

Other time-independent currents: Two other small currents were incorporated to maintain cardiomyocytes at -87 mV resting potential at all temperatures. Background sodium conductance (g_Nabg = 0.0000018 S/μF) is taken from Bondarenko et al.[15], while a temperature-dependent nonspecific current (i_ITEMP) was incorporated to offset small temperature variations in conductances near the resting potential, set at i_ITEMP = 0.0322 * {43 – (°C)} (pA/pF).

Cardiomyocyte strand simulations. The cardiomyocyte strands have a resting membrane potential of -87 mV. In all simulations, a 100 msec delay was employed to allow the Na_V Markov models to reach steady state prior to injecting the first cell with two 0.5 msec current stimuli at 10 Hz. Injected current amplitude was adjusted to achieve maximal induced sodium current in the first cell. The generated currents and voltages throughout the strand were analyzed only following the second stimulus, which takes into account the states of dynamic conductances at sinus rhythm. All simulations were conducted using Cvode multi-order variable time step integration method[16]. For each model, simulations were run after either elevating temperature in 1°C increments or reducing junctional, sodium, or calcium conductances in 1% increments. Conduction safety was defined as propagation of action potentials through the entire strand, with regenerative sodium current reaching steady cell-to-cell amplitude. Conduction failure was defined as a failure to generate sodium current in all cells throughout the strand with accompanying fall-off in depolarization amplitudes. In most simulations, conductance parameters were altered equivalently in all cells within the strand. However, to investigate how calcium conductance contributes to conduction safety in the *Fhf2*^{KO} strand, we conducted simulations where calcium conductance was deleted from cells 51-111 only.

Under any simulation condition, the *Fhf2*^{KO} cardiomyocytes generate substantially less sodium current than *Fhf2*^{WT} cardiomyocytes for two reasons: 1) at resting potential, approximately 74% of the sodium conductance is inactivated in *Fhf2*^{KO} cells, while there is only ~50% inactivation of the sodium conductance in *Fhf2*^{WT} cells (Figure 4E,F, Online Table VII), and 2) the Na_V model in *Fhf2*^{KO} cardiomyocytes has faster rates of closed-state and open-state inactivation than does the Na_v model in *Fhf2*^{WT} cells (Online Table VII). Action potential amplitudes, conduction velocity, [dV/dt]max, safety factor (SF), and conduction safety or failure thresholds in the *Fhf2*^{WT}and *Fhf2*^{KO} strands in response to variations of temperature, Gj, gNa_V, or gCa_V are summarized in Online Table VI. SF values were calculated based upon its originally described formulation[13], except that all membrane currents (sodium, calcium, potassium, capacitive) were incorporated into the calculation for determining when a cell transitioned from being predominantly a sink to a source[13].

The Graphical User Interface (GUI): The cardiomyocyte models have been uploaded onto ModelDB at https://senselab.med.yale.edu/modeldb/ in the NEURON simulation environment. Upon downloading and launching, a window in the GUI entitled "Set Sim Structure" allows for the selection of the *Fhf2*^{WT} or *Fhf2*^{KO} cardiomyocyte models, the temperature (37°C default), the number of myocytes in the strand (default 111), and the gap junctional conductance between cells along the strand (default 772,800 pS). Toggling between the WT and KO models alters the conductance densities for the Nav_withF and Nav_noF sodium channel models, and these densities are seen in the "Set Model Parameters" window. The selected strand model can be launched from the button "Linear Propagation Protocol", which generates additional windows,

including stimulus electrodes positioned within the first cell myocite.o[0] preset to generate 0.5 millisecond pulses of 30 nA at 100 msec and 200 msec after simulation initiation. The "Propagation Protocol" window allows selection of voltage vs. time, sodium current vs. time, and sodium channel states vs. time, and the simulation is initiated from the Run button.

In order to facilitate sodium current voltage clamp protocols, the "Set Sim Structure" window also has buttons to select for protocols to assay Na_v voltage dependence of activation, voltage dependence of steady-state inactivation, and sodium currents in response to variable-rate voltage ramps. The launch of any of these protocols creates a single cardiomyocyte with the selected genotype and temperature parameters, along with a protocol control window.

The densities of all ionic conductances can be changed equivalently in all cells of the strand using the Set Model Parameters window. This window can also be used to modify kinetic parameters for the sodium channel models. Changes to parameters of ionic and junctional conductances in a subset of cells within the strand can be made through hoc code commands in the terminal window. As examples,
1) The command:
for i=50,110 {prop_myo.myocites.o[i].cell.gcabar_Ca_L = 0}
sets the calcium conductance to zero in cells 51-111 of the strand (note that first cell in model is myocites.o[0])
2) The pair of commands:
prop_myo.gap_sources.o[10].g = 10000
prop_myo.gap_dests.o[10].g = 10000
resets the gap junctional conductance between cells 11 and 12 in the strand to 10000 pS.

Animal lines. All protocols conformed to the Association for the Assessment and Accreditation of Laboratory Animal Care and the NYU School of Medicine Animal Care and Use Committee. Mice used in this study were matched for age (7-18 weeks), sex (males) and genetic background. Mice carrying the Fhf2 KO[1] allele were backcrossed more than four generations to the 129/svPas strain before use in all cardiac physiology experiments. For gap junction uncoupling experiments, $Fhf2^{KO}$ mice were bred into the $Cx43^{flox/+}$; α-MHC-Cre line[17] to generate compound $Fhf2^{KO}$;Cx43 cardiac-specific heterozygous (cHet) mice. Mice carrying these three mutant alleles ($Fhf2^{KO}$, $Cx43^{flox/+}$, α-MHC-Cre) were backcrossed more than four generations to the 129/svPas strain before use in all cardiac physiology experiments. The following genotypes were used for each experimental group: 1) $Fhf2^{WT}$ ($Cx43^{flox/+}$); (2) Cx43 cHet ($Cx43^{flox/+}$, α-MHC-Cre); (3) $Fhf2^{KO}$ ($Fhf2^{KO/Y}$, $Cx43^{flox/+}$); (4) $Fhf2^{KO}$, Cx43 cHet ($Fhf2^{KO/Y}$, $Cx43^{flox/+}$, α-MHC-Cre). Animal lines were maintained by Charles River Laboratories; Wilmington, MA.

Antibody reagents. Immunofluorescence antibodies [target, dilution, (species, company)]. Primary antibodies: Cx43 1:100 (rabbit, Sigma Aldrich **C6219**), N-cad 1:100 (mouse, BD Biosciences, 610921). Mounting medium with DAPI (Vectashield, H-1200).

Cardiomyocyte enzymatic dissociation experiments. Performed as previously described by Park et al.[1] Cardiac cells were dissociated from adult hearts that were Langendorff perfused and enzymatically digested according to AfCS Procedure Protocols PP00000125. Mice were heparinized (500 U/kg) and euthanized with 100% carbon dioxide. Hearts were surgically removed via thoracotomy and immersed in ice cold perfusion buffer (composition [mmol/L]: 113 sodium chloride (NaCl), 4.7 potassium chloride (KCl), 0.6 potassium phosphate monobasic (KH_2PO_4), 0.6 sodium phosphate dibasic (Na_2HPO_4), 1.2 magnesium sulfate heptahydrate ($MgSO_4.7H_2O$), 12 sodium bicarbonate ($NaHCO_3$), 10 potassium bicarbonate (KHCO3), 10 HEPES buffer solution, 30 mM taurine, 5.5mM glucose, and 10 2,3-Butanedione monoxime (BDM)). The aorta was cannulated and Langendorff perfused with perfusion buffer at a constant flow rate of 3 ml/min for 3 minutes. The perfusate was then switched to myocyte dissociation buffer (composition:

1X perfusion buffer, 10mg Liberase TM, and 12.5μM calcium chloride ($CaCl_2$) at a constant flow rate of 3 ml/min for 8 minutes. Perfusate temperature was maintained at 37°C. Heart was removed, placed in a dish containing 2.5ml myocyte dissociation buffer plus 2.5ml stop buffer 1 (composition: 1X perfusion buffer, 10% Bovine calf serum (BCS), and 12.5μM calcium chloride ($CaCl_2$)), and tissue above the atrioventricular ring was removed. Ventricles were teased into several small pieces with fine forceps. Cellular dissociation was achieved by further, gentle mechanical agitation via 15ml transfer pipets. Quality of myocyte dissociation was then assessed by counting myocyte yield and percentage of rod-shaped myocytes. Only preparations with yields greater than 1 million cells and more than 60% rod-shaped myocytes were used for further experimentation. Cardiomyocytes were sedimented by centrifugation at 100 x g for 1 min in 15 ml tubes. The supernatant was discarded after sedimentation and the pellet was re-suspended in 10ml of stop buffer 2 (composition: 1X perfusion buffer, 5% Bovine calf serum (BCS), and 12.5μM calcium chloride ($CaCl_2$)) added to increasing concentration of Ca^{2+} in 5 minute intervals [+50 μl 10 mM Ca^{2+} (62 μM), +50 μl 10 mM Ca^{2+} (112μM), +100 μl 10 mM Ca^{2+} (212 μM), +30 μl 100 mM Ca^{2+} (500 μM), and +50 μl 100 mM Ca^{2+} (1 mM)]. Viability of myocytes was reassessed using the above quality control guidelines. Only cell preparations that passed these criteria were used for experimentation.

Immunohistochemistry. Mouse hearts were explanted and retrograde perfusion fixed in cold 4% PFA. Next, hearts were immersed in 4% PFA overnight (16 hours) at 4°C. Then samples were transferred for equilibration in 30% sucrose prepared with 1% PBS until the tissue sinks at 4°C. Hearts were then embedded in OCT and the frozen OCT blocks were stored at -80°C. OCT tissue blocks were cryosections in 8-10μM thick sections and mounted on microscope slides. Heart section slides were thawed at room temperature and then immediately placed in 1% PBS. Next, sections were blocked for 1 hour in 10% Normal Donkey Serum/0.1% Triton X-100, then incubated overnight (16 hours) at 4°C with the primary antibody. Slides were washed 3 times with 1% PBS and then incubation for 1 hr at room temperature with the secondary antibody. Slides were washed 3 times with 1% PBS and mounted with Vectashield plus DAPI for imaging.

Mouse electrocardiography (ECG) and drug challenge. ECGs were obtained using subcutaneous electrodes attached at the four limbs (MP100, BIOPAC Systems). Adult (7-18 week-old) male mice were anesthetized with inhaled (2% v/v) isoflurane. Heart rate and core body temperature (rectal temperature probe) were continuously recorded. Verapamil or carbenoxolone was administered via intraperitoneal injection. Experimentalists were not blinded in regard to drug administration nor animal genotype. ECG analysis was performed in an unbiased blinded fashion where 100 beats at each treatment endpoint were analyzed using LabChart 7 Pro version 7.3.1 (ADInstruments, Inc). Detection and analysis of P wave, PR interval, and QRS wave intervals were set to Mouse ECG parameters. Core body temperature was maintained at 37°C.

Heart isolation and Langendorff perfusion. 8–12 week-old, male mice were heparinized (500 U/kg) and euthanized with 100% carbon dioxide. Hearts were surgically removed *via* a thoracotomy. While fully immersed in oxygenated (95% O_2, 5% CO_2) Tyrode's (composition [mmol/L]: NaCl 114, $NaHCO_3$ 25, dextrose 10, KCl 4.6, $CaCl_2$ 1.5, Na_2PO_4 1.2, $MgCl_2$ 0.7), the aorta was cannulated and Langendorff perfused at a constant pressure of 70 mmHg. Perfusate temperature was maintained at 37°C.

Optical mapping. High-resolution optical mapping experiments were performed as follows: excised hearts from 8–12 week-old, male mice were initially perfused with Tyrode's solution to clear blood and stabilize the heart, followed by Tyrode's solution containing 10 microM blebbistatin. Hearts were allowed to recover for 20 min and then stained with the voltage-sensitive dye, Di-4-ANEPPS (Molecular Probes Inc., Eugene, OR, USA). Light from green LEDs (530 nm; ThorLabs) was used as an excitation source and the emitted light (620 nm long pass) was detected with 1 high-resolution CMOS camera (Mi-CAM Ultima-L;SciMedia)

at 1000 frames/s in bin mode (256x256 pixels) with 14-bit resolution. **Verapamil Infusion Studies:** After recording baseline maps, hearts were then infused with verapamil solution (0.25mg/L)[18] and reimaged. All images were processed using a custom software package.

A custom-made software package (adapted from[19]) written in MATLAB was used to analyze optical signals offline. Signal processing algorithm using FIR filter was adapted from an open source package[19]. In brief, time lapse fluorescence and ECG signals were acquired simultaneously using a single data acquisition system. The pixel resolution of the current optical mapping system is 48 microns per pixel. Detailed image processing algorithm is as follows: 1. Baseline wander and background noise were removed with a bandpass filter (FIR temporal filter with a band pass of 0–100 Hz). 2. For activation map generation, a single cycle is chosen by user on custom Graphic User Interface. Activation map was generated by measuring upstroke time of optical signals as described previously[20]. A 5 pixels x 5 pixels Gaussian averaging kernel was applied to reduce noise. 3. Conduction velocity (CV) was measured at a total of 12 radial angles with the step size of pi/6 radian around the pacing site, which was used as a focal reference. The gradient in activation maps represents the time taken by the activation front to travel a unit distance. The inverse of such gradient yields CV. The CV at each radial angle was obtained using linear regression model. Final CV from a given activation map was obtained by averaging CV obtained over all angles. Action potentials were averaged and normalized as previously reported[21]. APD was calculated at 50%, 75%, and 90% of repolarization (APD50, 75, and 90). Representative optical recordings can be found in Online Figure II.

Sodium current recordings in adult cardiomyocytes. All I_{Na} recordings in isolated cardiomyocytes were conducted in whole-cell configuration at 25°C. Recording pipettes were filled with a solution containing (in mM): NaCl 5, CsF 135, EGTA 10, MgATP 5, HEPES 15, pH 7.2 with CsOH. Cells were maintained in a solution containing (in mM): NaCl 5, CsCl 112.5, TEACl 20, $CdCl_2$ 0.1, $MgCl_2$ 1, $CaCl_2$, 1, HEPES 20, Glucose 11, pH 7.4 with CsOH. To determine the peak current voltage relation, 200 ms voltage pulses were applied to V_m -90 mV to +30 mV in 5 mV voltage steps, from a holding potential of V_m = -120 mV. Interval between voltage steps was 3 sec. From these data, peak sodium conductance density

$$g_{NavPeak} = I_{NavPeak}/(V_{com} - E_{Na}) \quad (1)$$

where E_{Na} is the sodium reversal potential and $I_{NavPeak}$ is the peak inward current in response to a voltage command V_{com} within the linear ohmic range of the current/voltage relationship. All recordings were obtained utilizing an Axon multiclamp 700B Amplifier coupled to a pClamp system (versions 10.2, Axon Instruments, Foster City, CA).

Calcium current recordings in adult cardiomyocytes. Ca^{2+} currents were recorded using the whole-cell patch-clamp configuration with the external recording solution of the following composition (in mM): 140 TEA-Cl, 10 CsCl, 10 Glucose, 10 HEPES, 1.0 $MgCl_2$, 1.2 $CaCl_2$, 2.0 4-AP, 0.03 TTX, pH 7.4 with CsOH. An internal pipette solution contained (in mM): 20 TEA-Cl, 120 CsCl, 10 HEPES, 5 EGTA, 5 Mg-ATP, 0.3 GTP, pH 7.2 with CsOH. Patch pipettes had mean resistances of 1.5–3 MΩ. All recordings were performed at room temperature (22–24 °C). Assessment of I_{Ca} density was obtained by holding the cell at −80 mV, followed by stepping to voltages between −60 and +40 mV, in 5 mV steps, for 400 ms, with 5 s interpulse intervals. From these data, peak calcium conductance density

$$G_{CavPeak} = I_{CavPeak}/(V_{com} - E_{Ca}) \quad (2)$$

where E_{Ca} is the calcium reversal potential and $I_{CavPeak}$ is the peak inward current in response to a voltage command V_{com} within the linear ohmic range of the current/voltage relationship. The decay of calcium current induced at -20 mV, -10 mV, and 0 mV was best-fitted to a two-component exponential decay with the formula

$$I_{Cav}(t) = I_{CavPeak} * (A_1 * e^{-t/Tau1} + A_2 * e^{-t/Tau2} + C) \quad (3)$$

where $I_{Cav}(t)$ is the calcium current at time t after $I_{CavPeak}$, Tau1 and Tau2 are time constants, A_1 and A_2 are the fractions of $I_{CavPeak}$ associated with the respective decay rates, and C is the nondecaying fraction. In order to determine voltage dependence of steady state calcium conductance inactivation, cells were depolarized from -100 mV holding potential to test voltages between -90 mV and +10 mV, in 5 mV steps for 500 ms, followed by further depolarization to reporting voltage of +15 mV, with 5 s interpulse intervals. The fraction of channels not inactivated at test voltage v equals $I_{CavPeak(v)}/I_{max}$, where I_{max} is $I_{CavPeak}$ upon direct depolarization from -100 mV to +15 mV.

Statistics.
Continuous variables were reported as medians and interquartile ranges except cellular electrophysiology data where means and standard error of the means are reported. The normality distribution was checked using Shapiro-Wilk test. When not normal, comparisons between two groups were made using Mann-Whitney U test, and Wilcoxon signed-rank test was performed for comparisons between paired samples. Additionally, the Kruskal-Wallis test was performed when comparing more than two groups of data followed by Benjamin-Hochberg post-hoc test for pairwise comparisons. To compare sodium and calcium current behavior in different genotypes, a two sample Kolmogorov-Smirnov test was used. A two-sided p-value <0.05 was considered to be statistically significant. Statistical analysis was performed with GraphPad Prism 8.0 software (San Diego, CA, USA) and Rstudio V3.5.2 (Foundation for Statistical Computing, Vienna, Austria). Itemized p-values can be found in Online Table VIII.

Representative Images. Representative images shown reflect the predominant phenotype.

Online Figure I

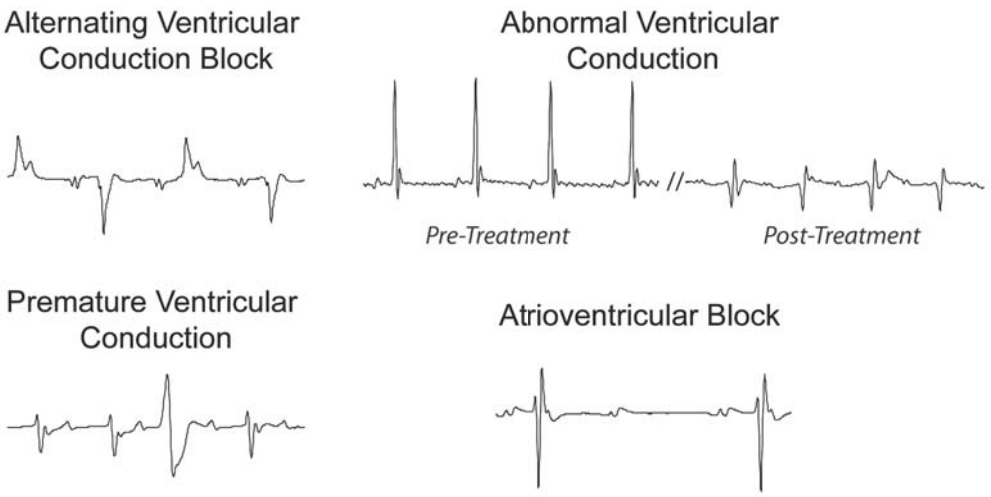

Online Figure I. ***In vivo*** **treatment of** ***Fhf2*** ^{KO} **mice with verapamil.** ECG features observed in *Fhf2* ^{KO} animals after verapamil challenge.

Online Figure II

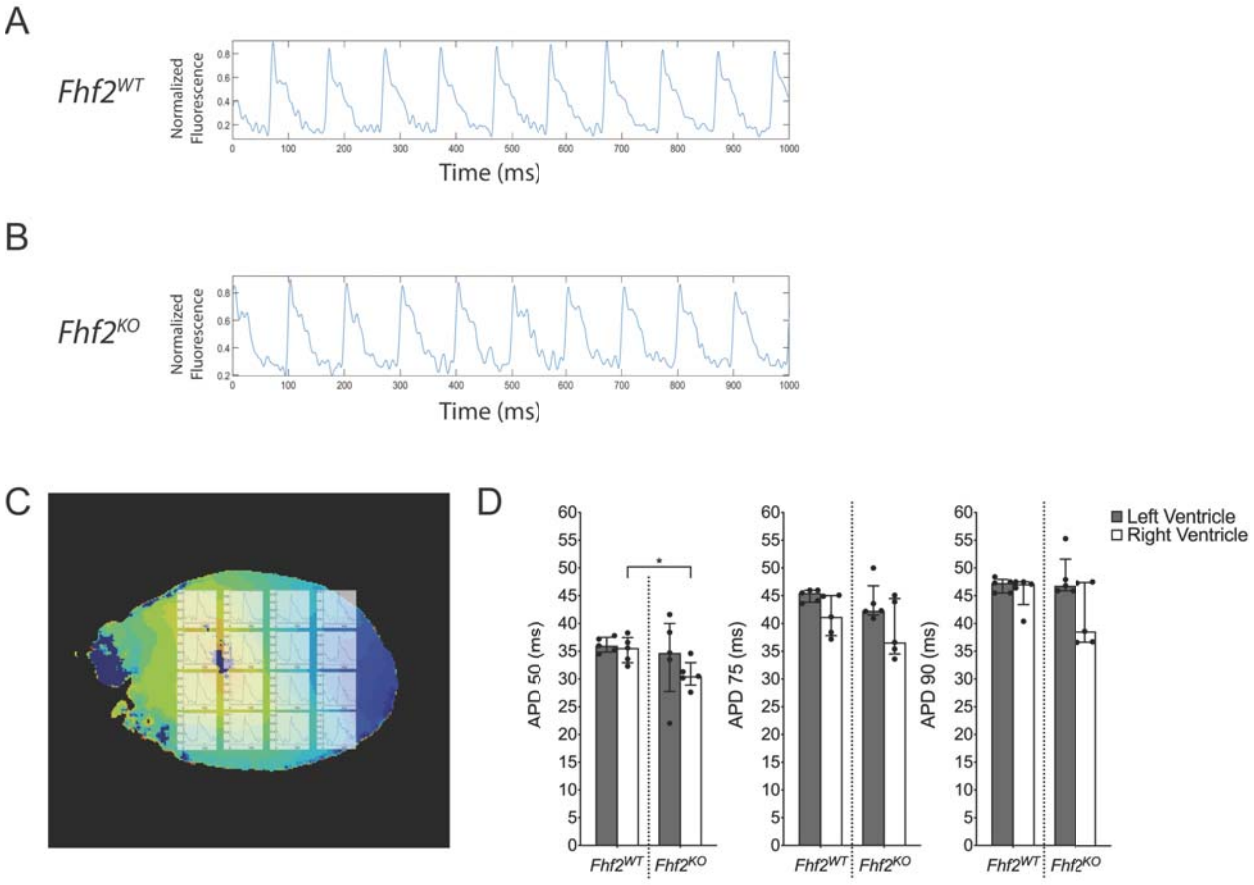

Online Figure II. (A) Representative optical recordings of Vm from *Fhf2*^{WT} left ventricle (LV). (B) Representative optical recordings of Vm from *Fhf2*^{KO} left ventricle (LV). (C) Representative optical recordings of Vm from different sites of the left ventricle. (D) Action potential duration (APD) 50, 75, and 90 in *Fhf2*^{WT} vs *Fhf2*^{KO} left and right ventricles paced at 100ms cycle length. n=5 animals per cohort. Data represent median ± interquartile range. *significant p values < 0.05, Wilcoxon signed-rank test was performed for comparisons between paired samples; Mann–Whitney U-test used for comparison of independent variables. See Online Table VIII for individual p-values.

Online Figure III

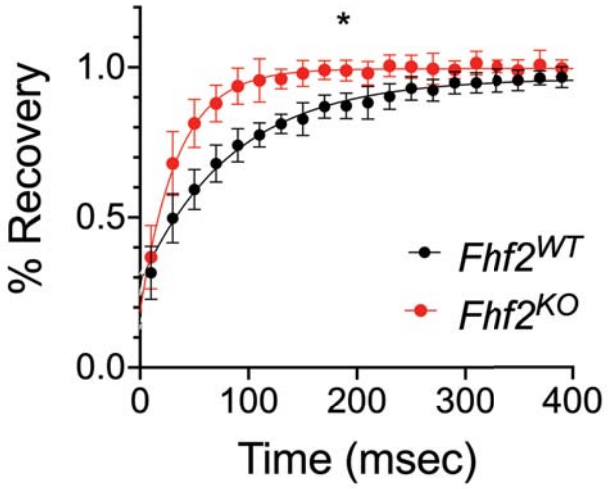

Online Figure III. Na_V recovery from inactivation is more rapid in *Fhf2*^{KO} cardiomyocytes. (n=3 mice per cohort; 3 cells/mouse). *significant p value < 0.0001; two-sample Kolmogorov-Smirnov test. See Online Table VIII for individual p-values.

Online Figure IV

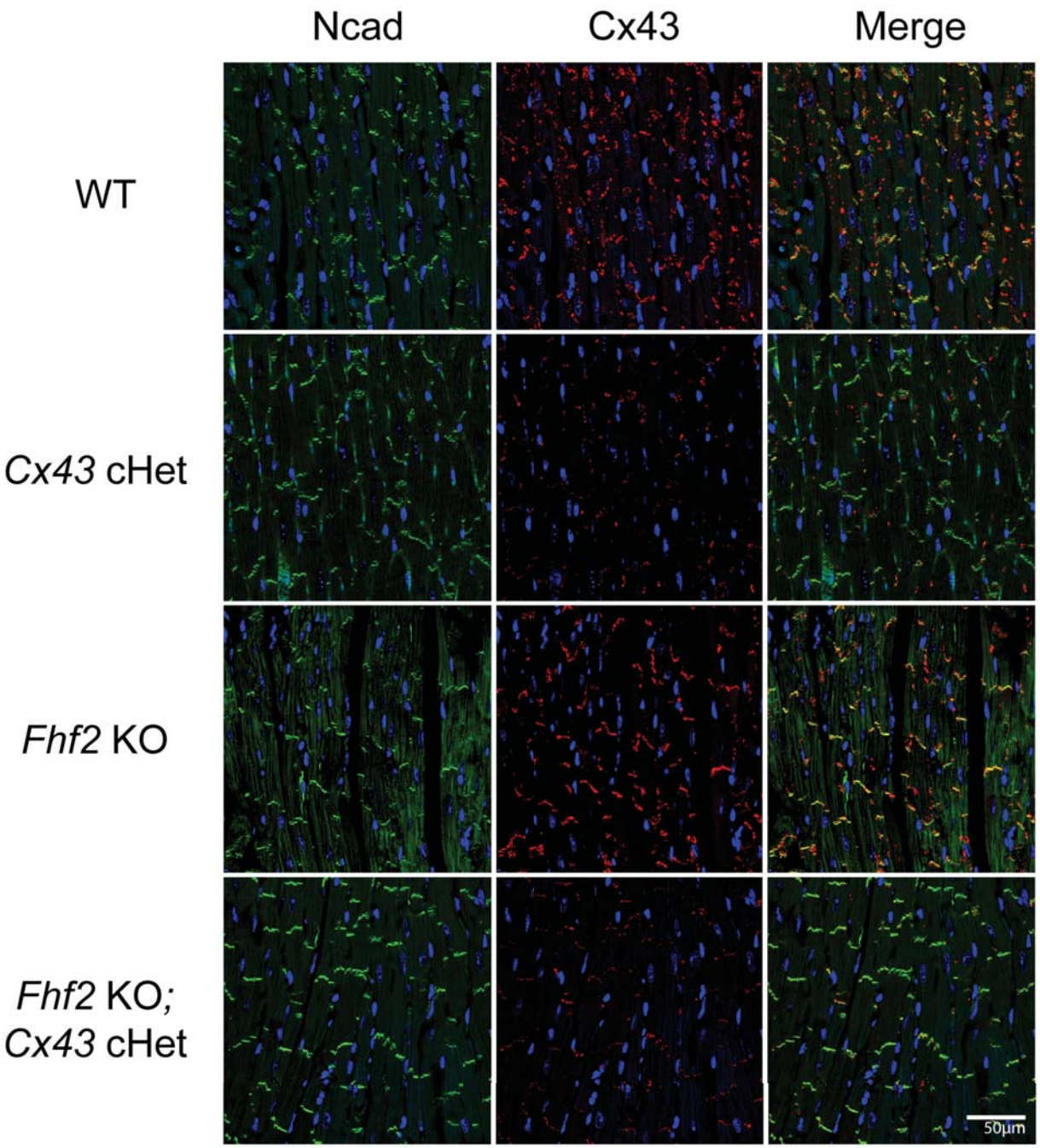

Online Figure IV. Immunofluorescence detection of Cx43 in $Fhf2^{WT}$, $Fhf2^{KO}$, Cx43 cHet, and $Fhf2^{KO}$;Cx43 cHet ventricular myocardium. Heart sections were fixed and probed with antibodies to N-cadherin (green) and Cx43 (red) along with DAPI (nuclear stain; blue). Loss of FHF2 does not affect Cx43 expression levels or localization to intercalated discs.

Online Figure V

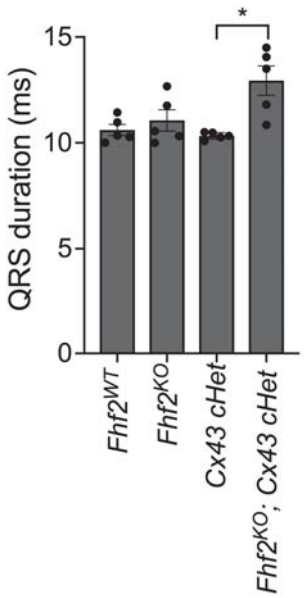

Online Figure V. Baseline electrocardiogram analysis of *Fhf2*^{KO};Cx43 cHet mice.
Fhf2^{KO};Cx43 cHet mice displayed prolonged QRS interval duration compared to *Fhf2*^{WT}, Cx43 cHet, and *Fhf2*^{KO} mice, although significance was only present with Cx43 cHet mice. n=5 animals per cohort. Data represent median ± interquartile range. *significant p values < 0.05; Mann–Whitney U-test. See Online Table VIII for individual p-values.

Online Figure VI

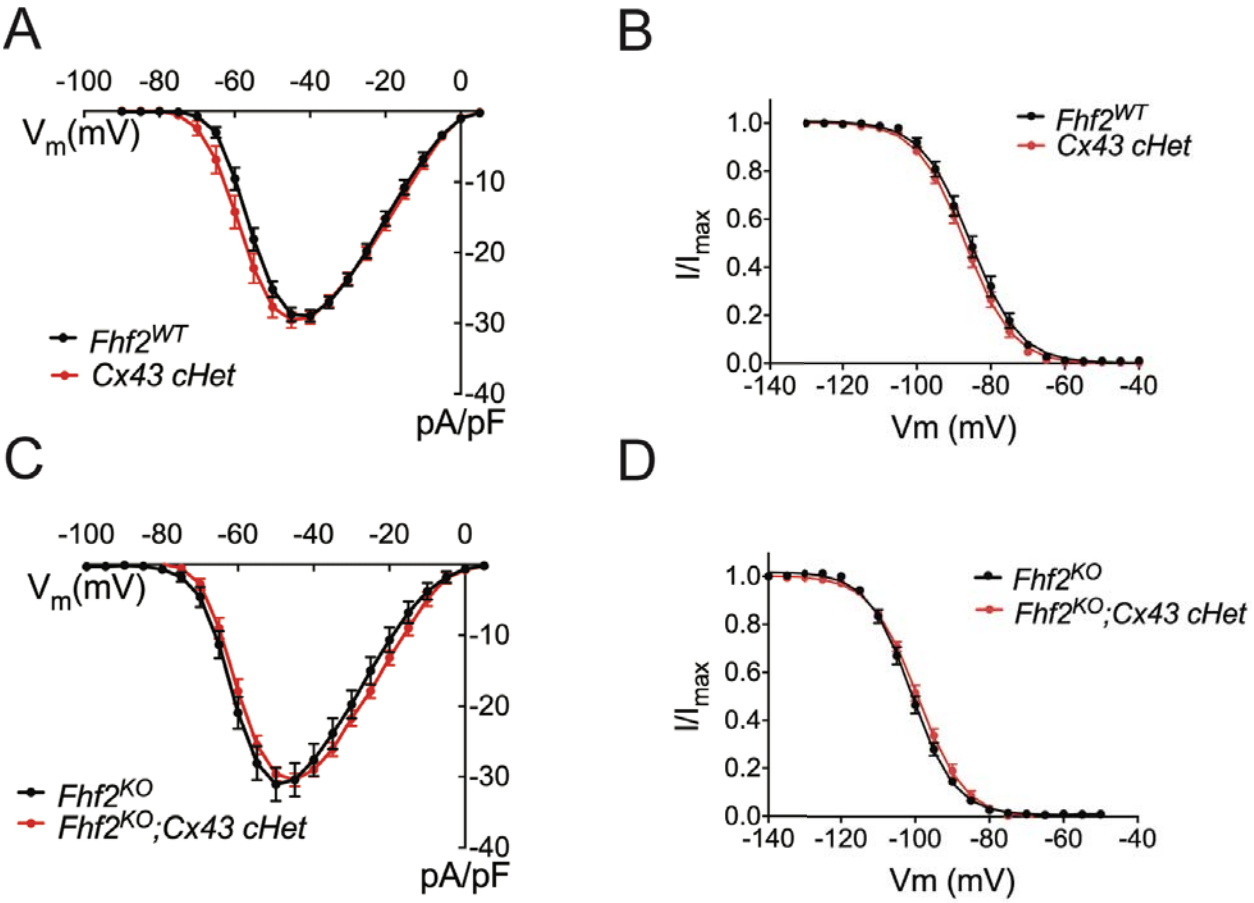

Online Figure VI. Measured sodium currents in *Fhf2^{WT}*, *Fhf2^{KO}*, Cx43 cHet, and *Fhf2^{KO}*;Cx43 cHet ventricular myocytes. (A) Sodium current density as a function of voltage in *Fhf2^{WT}* vs Cx43 cHet ventricular myocytes. *WT* and Cx43 cHet cardiomyocytes do not differ in the peak sodium current density. (B) Voltage-gated sodium channel steady-state inactivation. Available sodium currents are expressed as fraction of maximal current. Inactivation does not differ between *WT* and Cx43 cHet cardiomyocytes. (C) *Fhf2^{KO}* and *Fhf2^{KO}*;Cx43 cHet cardiomyocytes do not differ in the peak sodium current density. (D) Inactivation does not differ between *Fhf2^{KO}* and *Fhf2^{KO}*;Cx43 cHet cardiomyocytes. (n=3 mice in each cohort, 4 cells/mouse). Two-sample Kolmogorov-Smirnov test. See Online Table VIII for individual p-values.

Online Figure VII

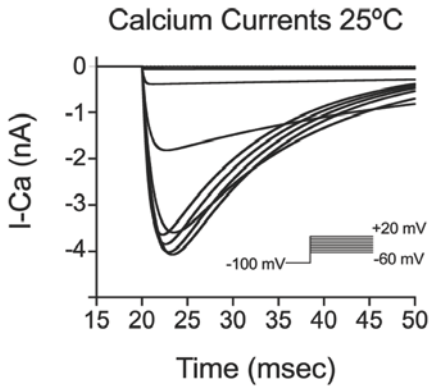

Online Figure VII. Calculated voltage gated calcium conductance for *Fhf2*^{WT} and *Fhf2*^{KO} cardiomyocytes. Current as a function of time.

Online Figure VIII

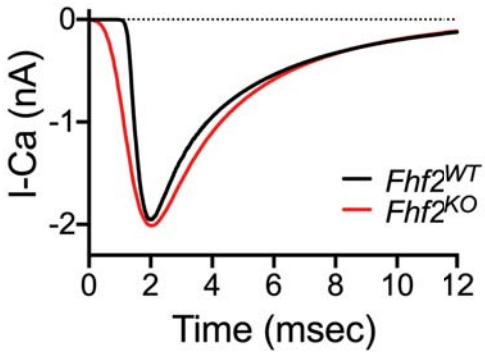

Online Figure VIII. Calcium currents are similar in individual *Fhf2*^{WT} and *Fhf2*^{KO} cells. Current as function of time in cell 50. During AP propagation, calcium currents are somewhat elevated in the *Fhf2*^{KO} compared to *Fhf2*^{WT} cell despite equivalent calcium conductances, due to the more negative voltage of the action potential in the *Fhf2*^{KO} cells.

Supplemental Tables

Genotype (Verapamil dose)	QRS (ms)
***Fhf2*^{WT} (0mg/kg)**	11.46 [10.85, 12.36]
***Fhf2*^{WT} (15mg/kg)**	11.59 [11.30, 11.82]
***Fhf2*^{KO} (0mg/kg)**	12.81 [12.25, 13.95]
***Fhf2*^{KO} (15mg/kg)**	24.49 [23.27, 25.64]

Online Table I. Cardiac conduction intervals in *Fhf2*^{WT} and *Fhf2*^{KO} mice treated with verapamil. Surface ECGs were obtained in adult *Fhf2*^{WT} and *Fhf2*^{KO} mice subjected to verapamil (0mg/kg or 15mg/kg) via intraperitoneal (IP) injection. n=4 for each genotype and dose combination. Data represent median ± interquartile range. See Online Table VIII for individual p-values.

Genotype (Verapamil)	LV (m/s)	RV (m/s)
Fhf2^{WT} **(0mg/L)**	0.64 [0.63, 0.67]	0.61 [0.60, 0.63]
Fhf2^{WT} **(0.25mg/L)**	0.60 [0.60, 0.67]	0.67 [0.64, 0.70]
Fhf2^{KO} **(0mg/L)**	0.27 [0.22, 0.28]	0.28 [0.27, 0.33]
Fhf2^{KO} **(0.25mg/L)**	Block	Block

Online Table II. Cardiac conduction velocity in *Fhf2^{WT}* and *Fhf2^{KO}* hearts treated with verapamil. Epicardial CV were measured in Langendorff perfused hearts before and after administration of verapamil. n=5 for each genotype. Data represent median ± interquartile range. See Online Table VIII for individual p-values.

Genotype	CV Min (m/s)	CV Max (m/s)	Anisotropic Ratio
Fhf2^{WT} (n=10)	0.42 [0.38, 0.45]	0.76 [0.66, 0.87]	1.78 [1.73, 1.91]
Fhf2^{WT} (Verapamil 0.25mg/L) (n=5)	0.43 [0.37, 0.43]	0.81 [0.80, 0.86]	1.90 [1.85, 2.17]
Fhf2^{KO} (n=5)	0.14 [0.13, 0.14]	0.42 [0.35, 0.42]	3.29 [3.11, 3.54]
Fhf2^{KO} (Verapamil 0.25mg/L) (n=5)	Block	Block	Block
Cx43 cHet (n=5)	0.39 [0.36, 0.39]	0.76 [0.75, 0.81]	2.10 [1.93, 2.26]
Fhf2^{KO};Cx43 cHet (n=5)	Block	Block	Block

Online Table III: Conduction velocity minimum (CV Min) and conduction velocity maximum (CV Max) and Anisotropic ratio. Data represent median ± interquartile range. Kruskal-Wallis test for more than two groups followed by Benjamin-Hochberg post-hoc test for pairwise comparisons. See Online Table VIII for individual p-values

Genotype (Carbenoxolone dose)	QRS (ms)
Fhf2^{WT} **baseline**	10.35 [10.28, 10.97]
Fhf2^{WT} **(60mg/kg)**	10.02 [9.84, 10.08]
Fhf2^{WT} **(90mg/kg)**	10.50 [10.40, 11.16]
Fhf2^{WT} **(120 mg/kg)**	10.19 [10.11, 10.70]
Cx43 cHet **baseline**	10.33 [10.26, 10.48]
Cx43 cHet **(60mg/kg)**	10.45 [10.00, 10.45]
Cx43 cHet **(90mg/kg)**	11.39 [10.76, 11.83]
Cx43 cHet **(120mg/kg)**	11.00 [10.95, 11.17]
Fhf2^{KO} **baseline**	10.56 [10.32, 11.76]
Fhf2^{KO} **(60mg/kg)**	13.07 [13.07, 13.21]
Fhf2^{KO} **(90mg/kg)**	14.50 [13.83, 14.89]
Fhf2^{KO} **(120mg/kg)**	15.83 [14.36, 15.94]
Fhf2^{KO}; Cx43 cHet **baseline**	13.50 [11.81, 14.06]
Fhf2^{KO}; Cx43 cHet **(60mg/kg)**	17.52 [13.32, 17.52]
Fhf2^{KO}; Cx43 cHet **(90mg/kg)**	16.84 [16.62, 17.63]
Fhf2^{KO}; Cx43 cHet **(120mg/kg)**	Lethal

Online Table IV. Cardiac conduction intervals in *Fhf2^{WT}*, Cx43 cHet, *Fhf2^{KO}*, and *Fhf2^{KO}*; Cx43 cHet mice treated with carbenoxolone. Surface ECGs were obtained in adult *Fhf2^{WT}*, *Cx43 cHet*, *Fhf2^{KO}*, and *Fhf2^{KO}; Cx43 cHet* mice at baseline and with increasing doses of carbenoxolone. n=5 for each genotype and dose combination. Data represent median ± interquartile range. See Online Table VIII for individual p-values.

Genotype	LV (m/s)	RV (m/s)
***Fhf2*^{WT}**	0.54 [0.53, 0.62]	0.61 [0.58, 0.65]
Cx43 cHet	0.53 [0.51, 0.54]	0.55 [0.55, 0.58]
***Fhf2*^{KO}**	0.24 [0.22, 0.27]	0.27 [0.25, 0.33]
***Fhf2*^{KO};Cx43 cHet**	Block	Block

Online Table V: Cardiac conduction velocity in *Fhf2*^{WT}, Cx43 cHet, *Fhf2*^{KO}, and *Fhf2*^{KO};Cx43 cHet. Baseline epicardial CV were measured in Langendorff perfused hearts. n=5 for each genotype. Data represent median ± interquartile range. See Online Table VIII for individual p-values.

	$Fhf2^{WT}$	$Fhf2^{KO}$	$Fhf2^{WT}$ Nav^{HYPO}	
AP Amplitude (mV)	39.7	16.8	22.2	
AP Conduction Velocity (m/sec)	0.475	0.339	0.346	
$[dV/dt]_{max}$ (mV/msec)	131	39	54	
Safety Factor	1.51	1.39	1.37	
Failure Temperature	*Safe at 45°C*	41°C	*Safe at 45°C*	
Failure at or below Gj (nS)	2.0	5.9	2.9	
Failure at gNav Fraction	0.21	0.68	0.42	
Failure at gCav Fraction	*Safe gCav=0*	0.54	*Safe gCav=0*	

Online Table VI. Action potential (AP) conduction properties in $Fhf2^{WT}$, $Fhf2^{KO}$, and $Fhf2^{WT}Nav^{HYPO}$ model strands. All conduction properties are from simulation at 37°C with Gj = 772.8 nS, unless indicated otherwise. All strands have a resting potential of -87 mV. The action potential conducts through the $Fhf2^{KO}$ strand with slower velocity and smaller amplitude than through the $Fhf2^{WT}$ strand due to greater sodium conductance steady state and dynamic inactivation in the $Fhf2^{KO}$ model. The $Fhf2^{KO}$ strand is more sensitive to conduction failure than the $Fhf2^{WT}$ strand in the face of elevated temperature or decrements in sodium, calcium, or junctional conductance. The sensitivities of the $Fhf2^{KO}$ strand are greater than those of the $Fhf2^{WT}Nav^{HYPO}$ strand, illustrating that the increases in both steady state and dynamic inactivation of sodium conductance contribute to the $Fhf2^{KO}$ strand phenotype.

	Model ***Fhf2^{WT}***	**Model** ***Fhf2^{WT}Nav^{HYPO}***	**Model** ***Fhf2^{KO}***	**Empirical** ***Fhf2^{WT}***	**Empirical** ***Fhf2^{KO}***
$V_{1/2}$ Steady State Inactivation (mV) 25°C	- 85.9	- 85.9	- 95.4	- 86.7 [a]	- 95.5 [a]
$V_{1/2}$ Steady State Inactivation (mV) 37°C	- 85.9	- 85.9	- 95.4	NT	NT
Slope Steady State Inactivation (mV) 25°C	7.1	7.1	7.5	6.3 [a]	7.5 [a]
Slope Steady State Inactivation (mV) 37°C	7.2	7.2	7.6	NT	NT
-135 mV to -30 mV Step I-Na_{peak} (pA/pF) 25°C	251	124	250	NA	NA
-87 mV to -30 mV Step I-Na_{peak} (pA/pF) 25°C	134	*67*	*67*	NA	NA
Open-State Inactivation Tau at -10 mV (ms) 25°C	2.04	2.04	1.55	2.36 [b]	1.50 [b]
Open-State Inactivation Tau at -10 mV (ms) 30°C	1.31	1.31	0.97	1.63 [b]	1.00 [b]
gNa_{peak} Ratio (5 mV/ms : V-step) 25°C	0.46	0.46	0.34	0.75 [b]	0.58 [b]
gNa_{peak} Ratio (5 mV/ms: V-step) 30°C	0.28	0.28	0.18	0.65 [b]	0.32 [b]
Fraction Recovered After 100 ms at -88 mV 25°C	0.79	0.79	0.94	0.76 [c]	0.94 [c]
Fraction Recovered After 100 ms at -100 mV 25°C	0.86	0.86	0.84	0.89 [c]	0.95 [c]
$V_{1/2}$ Activation (mV) 25°C	- 49.9	- 49.9	- 50.3	- 48.8 [a,c]	- 51.3 [a,c]

Online Table VII. Sodium conductance properties in *Fhf2*^{WT}, *Fhf2*^{KO}, and *Fhf2*^{WT}*Nav*^{HYPO} genetic models. The sodium conductances described in Scheme 1 were used in voltage clamp simulations. The behavior of the sodium conductance in *Fhf2*^{KO} model cardiomyocyte differs from that in the *Fhf2*^{WT} model cardiomyocyte in several key respects: hyperpolarizing shift in $V_{1/2}$ inactivation, faster inactivation from the open state at all temperatures, and greater closed state inactivation at all temperatures revealed by comparing peak conductance during a 5 mV/msec voltage ramp depolarization versus step depolarization. As shown in rows 1 and 2, $V_{1/2}$ steady-state inactivation is virtually temperature-independent since it represents an equilbrium property that does not substantially change as inactivation and recovery rates increase with rising temperature. The *Fhf2*^{WT}*Nav*^{HYPO} model was constructed by reducing gNa_v in the *Fhf2*^{WT} model such that I-Na_{peak} upon depolarization from -87 mV is equivalent to that of the *Fhf2*^{KO} model (row 6 italicized), while all Na_v gating properties of the *Fhf2*^{WT}*Nav*^{HYPO} model are identical to those of the *Fhf2*^{WT} model. Empirical data were described in: a, Wang et al. 2011[9]; b, Park et al. 2016[3]; c, this paper. NT, not tested empirically; NA, not applicable, as voltage-clamped sodium current recordings are measured at reduced extracellular sodium concentration.

Figure	Comparison	Test Used	Significance
1B	*Dose/Genotypes Comparisons*	Mann–Whitney U Test	
	Verapamil 0mg/kg: WT vs KO		n.s.
	Verapamil 15mg/kg: WT vs KO		p = 0.029
1D	*Interventricular Comparison (ie. LV vs RV)*	Wilcoxon	
	WT LV vs RV (Verapamil 0 mg/L)		n.s.
	WT LV vs RV (Verapamil 0.25 mg/L)		n.s.
	KO LV vs RV (Verapamil 0 mg/L)		n.s.
	KO LV vs RV (Verapamil 0.25 mg/L)		n/a (Block)
1D (cont.)	*Between Genotypes*	Mann–Whitney U Test	
	WT LV vs KO LV (Verapamil 0 mg/L)		p = 0.008
	WT RV vs KO RV (Verapamil 0 mg/L)		p = 0.008
2A	Calcium Current Density WT vs KO	Kolmogorov–Smirnov	n.s.
2B	Calcium Current Steady State Inact.	Kolmogorov–Smirnov	n.s.
Table 1	Tau (Calcium Current Inactivation) -20mV: Tau1, Tau1Frac, Tau2,Tau2Frac: WT vs KO -10mV: Tau1, Tau1Frac, Tau2,Tau2Frac: WT vs KO -0mV: Tau1, Tau1Frac, Tau2,Tau2Frac: WT vs KO	Mann–Whitney U Test	n.s.
3B	*Between Genotypes*[a]	Kruskal–Wallis Test; Benjamin–Hochberg Post Hoc Test	
	cHet vs KO/cHet (CBX 0mg/kg)		p = 0.048
	KO vs cHet (CBX 60mg/kg)		p = 0.018
	KO vs KO/cHet (CBX 60mg/kg)		p = 0.042
	KO vs WT (CBX 60mg/kg)		p = 0.018
	KO/cHet vs WT (CBX 60mg/kg)		p = 0.018
	KO/cHet vs cHet (CBX 60mg/kg)		p = 0.018
	KO vs cHet (CBX 90mg/kg)		p = 0.0095
	KO vs KO/cHet (CBX 90mg/kg)		p = 0.0095
	KO vs WT (CBX 90mg/kg)		p = 0.0095
	cHet vs KO/cHet (CBX 90mg/kg)		p = 0.0095
	KO/cHet vs WT (CBX 90mg/kg)		p = 0.0095
	KO vs cHet (CBX 120mg/kg)		p = 0.012
	KO vs WT (CBX 120mg/kg)		p = 0.012
3B (cont.)	*Dose Comparison: Individual Genotypes (CBX mg/kg)*	Kruskal–Wallis Test; Benjamin–Hochberg Post Hoc Test	
	WT (0 vs 60 vs 90 vs 120)		n.s.
	cHet (0 vs 60 vs 90 vs 120)[b]		p = 0.04
	KO (0 vs 60 vs 90 vs 120) 0 vs 60 0 vs 90 0 vs 120 60 vs 90 60 vs 120		p = 0.001 p = 0.032 p = 0.024 p = 0.024 p = 0.043 p = 0.024

	KO/cHet (0 vs 60 vs 90 vs 120) 0 vs 90		p = 0.049 p = 0.024
3D	*Interventricular Comparison (ie. LV vs RV)*	Wilcoxon	
	WT LV vs RV		n.s.
	KO LV vs RV		n.s.
	cHet LV vs RV		n.s.
3D (cont.)	*Between Genotypes*	Kruskal–Wallis Test; Benjamin–Hochberg Post Hoc Test	
	Left Ventricle: WT LV vs KO LV vs cHet LV KO LV vs cHet LV KO LV vs WT LV WT LV vs cHet LV		p = 0.006 p = 0.012 p = 0.012 p = n.s.
	Right Ventricle: WT RV vs KO RV vs cHet RV KO RV vs cHet RV KO RV vs WT RV WT RV vs cHet RV		p = 0.009 p = 0.024 p = 0.024 p = n.s.
Online Fig IID	*Interventricular Comparison (ie. LV vs RV)* APD 50: WT LV vs RV APD 50: KO LV vs RV APD 70: WT LV vs RV APD70: KO LV vs RV APD90: WT LV vs RV APD90: KO LV vs RV	Wilcoxon	n.s.
Online Fig IID (cont.)	*Between Genotypes* APD 50: WT LV vs KO LV APD 50: WT RV vs KO RV APD 70: WT LV vs KO LV APD 70: WT RV vs KO RV APD 90: WT LV vs KO LV APD 90: WT RV vs KO RV	Mann–Whitney U Test	n.s. p = 0.031 n.s. n.s n.s n.s.
Online Fig III	*Na_V recovery from inactivation: WT vs KO*	Kolmogorov–Smirnov	p < 0.0001
Online Fig V	*Baseline QRS (WT vs KO vs cHet vs KO/cHet)* cHet vs KO/cHet	Kruskal–Wallis Test; Benjamin–Hochberg Post Hoc Test	p = 0.031 p = 0.048
Online Fig VIA	Sodium Current Density (WT vs cHet)	Kolmogorov–Smirnov	n.s.
Online Fig VIB	Voltage Dependence of Inactivation (WT vs cHet)	Kolmogorov–Smirnov	n.s.
Online Fig VIC	Sodium Current Density (KO vs KO/cHet)	Kolmogorov–Smirnov	n.s.
Online Fig VID	Voltage Dependence of Inactivation (KO vs KO/cHet)	Kolmogorov–Smirnov	n.s.
Online Table III	*CV Min (WT vs WT+Verapamil vs KO vs cHet)* *$Fhf2^{KO}$* vs *$Fhf2^{WT}$* *$Fhf2^{KO}$* vs *$Fhf2^{WT}$* + Verapamil *$Fhf2^{KO}$* vs Cx43 cHet	Kruskal–Wallis Test; Benjamin–Hochberg Post Hoc Test	p = 0.003 p = 0.004 p = 0.016 p = 0.016

Online Table III (con't)	*CV Max (WT vs WT+Verapamil vs KO vs cHet)* *Fhf2*^{KO} vs *Fhf2*^{WT} *Fhf2*^{KO} vs *Fhf2*^{WT} + Verapamil *Fhf2*^{KO} vs Cx43 cHet	Kruskal–Wallis Test; Benjamin–Hochberg Post Hoc Test	p = 0.008 p = 0.004 p = 0.016 p = 0.016
Online Table III (con't)	*Anisotropic Ratio (WT vs WT+Verap vs KO vs cHet)* *Fhf2*^{KO} vs *Fhf2*^{WT} *Fhf2*^{KO} vs *Fhf2*^{WT} + Verapamil *Fhf2*^{KO} vs Cx43 cHet *Fhf2*^{WT} vs Cx43 cHet	Kruskal–Wallis Test; Benjamin–Hochberg Post Hoc Test	p = 0.002 p = 0.004 p = 0.016 p = 0.016 p = 0.042

[a] Only significant comparisons are listed given number of statistical tests performed
[b] No comparisons were significant after Benjamin–Hochberg Post Hoc Test

Online Table VIII. Individual p-values for statistical comparisons of all figures. WT, *Fhf2* wildtype; KO, *Fhf2* knockout; cHet, cardiomyocyte-selective Cx43 heterozygous (Cx43 cHet); LV, left ventricle, RV, right ventricle; APD, action potential duration; CBX, carbenoxolone; n.s., not significant.